Joint Beamforming and Antenna Selection for Two-Way Amplify-and-Forward MIMO Relay Networks

Gayan Amarasuriya, Chintha Tellambura and Masoud Ardakani
Department of Electrical and Computer Engineering, University of Alberta, Edmonton, AB, Canada T6G 2V4
Email: {amarasur, chintha, ardakani}@ece.ualberta.ca

***Abstract*—A novel joint beamforming and antenna selection strategy is proposed and analyzed for two-way multiple-input multiple-output amplify-and-forward relay networks. Specifically, this strategy selects the optimal transmit precoding and receiver filtering vectors at the two source terminals, and an optimal transmit/receive antenna at the relay terminal based on minimizing the overall outage probability. The performance of this transmission strategy is quantified by first deriving the exact cumulative distribution function of the effective signal-to-noise ratio (SNR), and thereby, evaluating the overall outage probability, its asymptotically exact high SNR approximation and achievable diversity order. For a multiple relay scenario, a joint relay, beamforming, and antenna selection strategy is proposed and analyzed as well. Interestingly, our selection strategies are optimal in the sense of the overall outage probability, and hence, in the sense of achievable diversity order as well.**

I. Introduction

Two-way relay networks (TWRNs) have recently been gaining significant attention due to their superior performance over conventional one-way relay networks (OWRNs) [1]–[4]. In fact, OWRNs require four orthogonal channel uses to exchange two messages between two sources via a relay, whereas TWRNs achieve the same objective by using just two orthogonal channel uses. Thus, TWRNs avoid the pre-log factor of one-half in capacity expressions, and hence, are twice as spectral efficient as OWRNs [2], [3]. In particular, multiple-input multiple-output (MIMO) technologies can be used effectively to further enhance the performance of single-antenna TWRNs [5]–[10]. Specifically, transmit precoding and receive filtering (a.k.a. beamforming) in terms of maximal ratio transmission (MRT) and maximal ratio combining (MRC), respectively, improve the performance of such networks, because of their robustness against severe fading effects [11]. Further, antenna selection reduces the complexity and power requirements, and hence, the cost of the MIMO transceivers by eliminating the need of multiple transmit and receive radio frequency (RF) chains [12]. Thus, in this paper, a novel joint beamforming and antenna selection strategy, which is optimal in the sense of achievable diversity order, is proposed and analyzed for MIMO amplify-and-forward (AF) TWRNs.

Prior related research: The precoder/decoder design for MIMO AF TWRNs is studied in [5]–[10]. In [5], the optimal relay beamforming structure is derived and used to study the achievable capacity regions. Further, [6] designs optimal relay precoders for multi-relay TWRNs, and thereby, studies the sum-rate and average bit error rate (BER). In both [3] and [6], multiple-antennas are employed only at the relays, whereas both sources are single-antenna terminals. Reference [7] quantifies the detrimental impact of channel estimation errors for MIMO receiver designs. In [8], the MIMO transceiver processing is optimized by using zero forcing and minimum square mean error techniques. In [9], [10], optimal relay beamforming structures are derived based on the weighted sum-rate optimization criteria. All the aforementioned studies [5]–[10] involve convex optimization techniques for designing MIMO precoders/decoders of AF TWRNs.

Only few studies, [13]–[15], dealing with antenna selection issue for MIMO AF TWRNs have been published. In [13], upper bounds for the average BER of network-coded TWRNs having two single-antenna sources and a dual-antenna relay are studied. Further, [14] extends [13] by using either max-min antenna selection or MRT in the second time-slot. In [15], we studied the best transmit/receive (Tx/Rx) antenna pair selection for MIMO AF TWRNs.

Motivation and our contribution: Although [3], [6]–[8] derive beamforming structures for MIMO TWRNs, they do not render themselves useful for deriving closed-form performance metrics such as the outage probability and diversity order due to the complicated MIMO precoder/decoder designs resulted from convex optimization theory. In particular, these precoder/decoder designs at the relay require employing multiple Tx/Rx RF chains, and hence, increase both complexity and cost[1]. This situation clearly loosens one of the main trade-offs of deploying relay networks; i.e., the cost versus performance. Moreover, [13] and [14] study the antenna selection only for the decode-and-forward TWRNs, where individual symbols from the two sources are first decoded separately and then a network-coded symbol is broadcast back to two sources. Specifically, the system models in both [13][2] and [14] consist of multiple antennas at the relay only, whereas each source is equipped with a single antenna. Further, they consider transmit antenna selection during the second time-slot (broadcast phase) only.

Therefore, to the best of our knowledge, both joint beamforming and Tx/Rx antenna selection for single-relay MIMO AF TWRNs and joint beamforming, antenna, and relay selection for multi-relay MIMO AF TWRNs have not yet been studied. Thus, this paper fills this gap by proposing and

[1]The passive antenna terminals and additional digital signal processing circuitry are becoming increasingly cheaper, however, RF elements are still expensive and do not follow Moore's law [12].

[2]The system model in [13] is restricted to a dual-antenna relay terminal.

978-1-4577-2053-6/12/$31.00 ©2012 IEEE

analyzing a new joint beamforming and antenna selection strategy for MIMO AF TWRNs. Specifically, we consider all MIMO-enabled terminals and the proposed transmission strategy jointly selects the optimal transmit precoding and receiver filtering vectors at the two sources and the best Tx/Rx antenna at the relay based on minimizing the overall outage probability while retaining the full diversity order. Furthermore, the multi-relay scenario is also treated by proposing and analyzing a joint beamforming and antenna/relay selection strategy. Notably, the performance of the proposed transmission strategies is quantified by deriving closed-form expressions for the exact overall outage probability, its high SNR approximation and diversity order. Further, numerical results and Monte-Carlo simulations are provided to show the performance gains, and to validate our analysis, respectively. Our analysis reveals that our selection strategies are optimal in the sense of diversity order, and hence, are useful in practical designs of MIMO AF TWRNs.

II. System model

We consider a half-duplex MIMO AF TWRN consisting of two source terminals (S_1 and S_2), and a relay terminal (R). Specifically, S_1, S_2 and R are equipped with N_1, N_2 and N_R antennas, respectively. All channel amplitudes are assumed to be frequency-flat and independently distributed Rayleigh fading. Full channel state information is assumed to be available at all terminals and feedbacks for beamforming and antenna selection are assumed to be perfect unless otherwise stated. The channel matrix from S_i to R is denoted by $\mathbf{H}_{S_iR} \in \mathcal{C}^{N_r \times N_i}$ for $i = 1, 2$ having entires as $h_{S_iR}^{(k,l)} \sim \mathcal{CN}(0, \zeta_i)$, where ζ_i accounts for the path-loss effect and modeled as $\zeta_i \propto (d_{S_iR})^{-\delta}$. Here, d_{S_iR} is the distance between S_i and R, and δ is the path-loss exponent. In particular, all the channels are assumed to be fixed over two consecutive time-slots [2]. Thus, the channel matrix from R to S_i (i.e., $\mathbf{H}_{RS_i}$) can be denoted as $(\mathbf{H}_{S_iR})^T$. The direct channel between S_1 and S_2 is assumed to be unavailable due to heavy path-loss and shadowing.

In the first time-slot, both S_1 and S_2 transmit their information-bearing symbols[3], $\mathcal{X}_1$ and $\mathcal{X}_2$, simultaneously by using MRT transmit precoding vectors corresponding to the j-th receive antenna at R over a multiple access channel. The superimposed-signal received at the j-th receive antenna of R is given by

$$Y_R^{(j)} = \sqrt{\mathcal{P}_1} h_{S_1R}^{(j)} U_1^{(j)} \mathcal{X}_1 + \sqrt{\mathcal{P}_2} h_{S_2R}^{(j)} U_2^{(j)} \mathcal{X}_2 + n_R, \quad (1)$$

where $h_{S_iR}^{(j)} \in \mathcal{C}^{1 \times N_i}$ for $i = 1, 2$ is the channel vector from all N_i transmit antenna of S_i to j-th receive antenna of R. Further, $U_i^{(j)} \in \mathcal{C}^{N_i \times 1}$ is the transmit beamforming vector at S_i and given by $U_i^{(j)}\Big|_{i=1}^2 = \left(h_{S_iR}^{(j)}\right)^H / \left|\left|h_{S_iR}^{(j)}\right|\right|$. In (1), $\mathcal{P}_i\big|_{i=1}^2$ is the transmit power of S_i and n_R is the additive white Gaussian noise (AWGN) at the j-th antenna of R with mean zero and variance σ_R^2.

[3]The information-bearing symbols have unit symbol energies, i.e., $\mathcal{E}\{|\mathcal{X}_1|^2\} = 1$ and $\mathcal{E}\{|\mathcal{X}_2|^2\} = 1$.

In the second time slot, the j-th antenna of R amplifies $Y_R^{(j)}$ with a gain $G = \sqrt{\frac{\mathcal{P}_R}{\mathcal{P}_1\left|\left|h_{S_1R}^{(j)}\right|\right|^2 + \mathcal{P}_2\left|\left|h_{S_2R}^{(j)}\right|\right|^2 + \sigma_R^2}}$ and then broadcast it again by using the j-th transmit antenna to $S_i\big|_{i=1}^2$ over the broadcast channel. Here, $\mathcal{P}_R$ is the transmit power at R. Then, S_1 and S_2 combine the signal by using the MRC receive filtering vectors $V_1^{(j)}$ and $V_2^{(j)}$, respectively, as follows:

$$Y_{S_i}\big|_{i=1}^2 = V_i^{(j)} \left[G Y_R^{(j)} \left(h_{S_iR}^{(j)}\right)^T + n_i\right], \quad (2)$$

where $n_i\big|_{i=1}^2$ is the AWGN at S_i having mean zero and variance σ_i^2. Specifically, the receive filter vectors are constructed as $V_i^{(j)}\Big|_{i=1}^2 = \left(h_{S_iR}^{(j)}\right)^\dagger / \left|\left|h_{S_iR}^{(j)}\right|\right|$.

By substituting (1) into (2) and removing the self-interference[4] [2], the end-to-end signal-to-noise ratio (e2e SNR) at $S_i\big|_{i=1}^2$ can be derived as

$$\gamma_{S_1}^{(j)} = \frac{\left(\frac{\mathcal{P}_R\left|\left|h_{S_1R}^{(j)}\right|\right|^2}{\sigma_1^2}\right)\left(\frac{\mathcal{P}_2\left|\left|h_{S_2R}^{(j)}\right|\right|^2}{\sigma_R^2}\right)}{\left(\frac{\mathcal{P}_R}{\sigma_1^2} + \frac{\mathcal{P}_1}{\sigma_R^2}\right)\left|\left|h_{S_1R}^{(j)}\right|\right|^2 + \frac{\mathcal{P}_2\left|\left|h_{S_2R}^{(j)}\right|\right|^2}{\sigma_R^2} + 1} \quad \text{and}$$

$$\gamma_{S_2}^{(j)} = \frac{\left(\frac{\mathcal{P}_1\left|\left|h_{S_1R}^{(j)}\right|\right|^2}{\sigma_2^2}\right)\left(\frac{\mathcal{P}_R\left|\left|h_{S_2R}^{(j)}\right|\right|^2}{\sigma_R^2}\right)}{\frac{\mathcal{P}_1\left|\left|h_{S_1R}^{(j)}\right|\right|^2}{\sigma_R^2} + \left(\frac{\mathcal{P}_R}{\sigma_2^2} + \frac{\mathcal{P}_2}{\sigma_R^2}\right)\left|\left|h_{S_2R}^{(j)}\right|\right|^2 + 1}. \quad (3)$$

In the next section, the optimal selection of relay antenna index, j, is described in detail.

III. Problem formulation

In this section, the optimal joint beamforming and antenna selection strategy for MIMO AF TWRNs is formulated. Our key objective is to minimize the overall outage probability by jointly selecting the optimal transmit precoding and receive filtering vectors at $S_i\big|_{i=1}^2$ and the optimal Tx/Rx antenna at R. In fact, the overall performance of multiuser systems is governed by the performance of the weakest source [16], and hence, our system is in outage if either S_1 or S_2 is in outage. This motivates our key design criterion, which is to jointly maximize the e2e SNR of the weakest source, and thereby, minimize the overall outage probability. To this end, the optimal Tx/Rx antenna terminal at R, and the optimal bemaforming vectors at S_i are selected as follows:

$$\{J\} = \underset{1 \le j \le N_R}{\operatorname{argmax}} \left[\min\left(\gamma_{S_1}^{(j)}, \gamma_{S_2}^{(j)}\right)\right], \quad (4)$$

where J is the optimal antenna index at R, and the corresponding optimal transmit precoding and receive filtering vectors at $S_i\big|_{i=1}^2$ are derived by using MRT and MRC principles as $U_i^{(J)}\Big|_{i=1}^2 = \left(h_{S_iR}^{(J)}\right)^H / \left|\left|h_{S_iR}^{(J)}\right|\right|$ and $V_i^{(J)}\Big|_{i=1}^2 = \left(h_{S_iR}^{(J)}\right)^\dagger / \left|\left|h_{S_iR}^{(J)}\right|\right|$, respectively[5].

[4]It is assumed that S_i knows its own information-bearing symbol $\mathcal{X}_i$ and all the channel coefficients.

[5]Here. $(\cdot)^H$ and $(\cdot)^\dagger$ denote the complex conjugate transpose and complex conjugate operators, respectively.

IV. Outage Probability Analysis

In this section, the exact overall outage probability is derived. Specifically, an asymptotically exact high SNR approximation of the outage probability is also derived, and thereby, valuable insights into practical system design are obtained in terms of the diversity order.

A. Overall outage probability

The overall outage probability, P_{out}, is defined as the probability that the instantaneous e2e SNR of the weakest source terminal falls below the preset threshold γ_{th}[6]. Thus, P_{out} is given by

$$P_{out} = \Pr\left[Z = \max_{1\leq j\leq N_R}\left\{\min\left(\gamma_{S_1}^{(j)}, \gamma_{S_2}^{(j)}\right)\right\} \leq \gamma_{th}\right]. \quad (5)$$

Specifically, P_{out} in (5) can be derived in closed-form by evaluating the cumulative distribution function (CDF) of the random variable Z at γ_{th} as follows (see the Appendix for the proof):

$$P_{out}{=}F_Z(\gamma_{th}){=}\left[\Psi_{N_1,N_2,\zeta_1,\zeta_2}(\gamma_{th}){+}\Psi_{N_2,N_1,\zeta_2,\zeta_1}(\gamma_{th})\right]^{N_R}, (6)$$

where $\Psi_{M,N,a,b}(z)$ is given by (7) in the top of the next page. In (7), $\alpha = \frac{\bar{\gamma}_S+\bar{\gamma}_R}{\bar{\gamma}_R\bar{\gamma}_T}$, $\beta = \frac{1}{\bar{\gamma}_R}$, $\eta = \frac{1}{\bar{\gamma}_S\bar{\gamma}_S}$ and $\phi(z) = \frac{1}{\bar{\gamma}_S\bar{\gamma}_R}\sqrt{(\bar{\gamma}_S^2 + \bar{\gamma}_S\bar{\gamma}_R + \bar{\gamma}_R^2/4)z^2 + \bar{\gamma}_S\bar{\gamma}_R z + \frac{z}{2\bar{\gamma}_S}}$.

B. High SNR approximation of the overall outage probability

In this subsection, an asymptotically exact high SNR approximation of the overall outage probability is derived, and thereby, the achievable diversity order is quantified.

The asymptotic outage probability at high SNRs is derived as (see the Appendix for the proof)

$$P_{out}^{\infty} = \Delta\left(\frac{\gamma_{th}}{\bar{\gamma}}\right)^{G_d} + o\left(\bar{\gamma}^{-(G_d+1)}\right), \quad (8)$$

where the diversity order, G_d, is given by

$$G_d = N_R \min(N_1, N_2). \quad (9)$$

The system-dependent parameter Δ in (8) is given by

$$\Delta{=}\begin{cases}\frac{1}{[\Gamma(N_1{+}1)]^{N_R}}\left(\frac{\mu_S+\mu_R}{\zeta_1\mu_S\mu_R}\right)^{N_1N_R}, & N_1<N_2\\ \frac{1}{[\Gamma(N{+}1)]^{N_R}}\left(\frac{1}{\zeta_1^N}+\frac{1}{\zeta_2^N}\right)^{N_R}\left(\frac{\mu_S+\mu_R}{\mu_S\mu_R}\right)^{NN_R}, & N_1{=}N_2{=}N\\ \frac{1}{[\Gamma(N_2{+}1)]^{N_R}}\left(\frac{\mu_S+\mu_R}{\zeta_2\mu_S\mu_R}\right)^{N_2N_R}, & N_1>N_2,\end{cases} \quad (10)$$

where μ_S and μ_R are the ratios of the source and relay average transmit SNR to the reference average transmit SNR ($\bar{\gamma}$), respectively, i.e., $\mu_S = \frac{\bar{\gamma}_S}{\bar{\gamma}}$ and $\mu_R = \frac{\bar{\gamma}_R}{\bar{\gamma}}$.

V. Joint relay and antenna selection

In this section, our proposed joint beamforming and antenna selection strategy is extended to two-way MIMO AF multi-relay networks. Specifically, our system model consists of two source terminals, S_1 and S_2, and K number of potential relays ($R_k|_{k=1}^{K}$), each equipped with N_1, N_2 and $N_{R_k}|_{k=1}^{K}$ antennas, respectively. Our design objective is to maximize the e2e SNR of the weakest source, and hence, minimize the overall outage probability by jointly selecting the best relay, its best antenna and the corresponding transmit precoding and receive filtering vectors at the two source terminals. Thus, this selection strategy is formulated as

$$\{K^{\circledast}, J_{K^{\circledast}}\} = \underset{\substack{1\leq j\leq N_{R_k}\\ 1\leq k\leq K}}{\operatorname{argmax}}\left[\min\left(\gamma_{S_1}^{(j_k)}, \gamma_{S_2}^{(j_k)}\right)\right], \quad (11)$$

where $K^{\circledast}$ and $J_{K^{\circledast}}$ are the optimal relay index and its optimal Tx/Rx antenna index, respectively. The corresponding transmit precoding and receive filtering vectors at $S_i|_{i=1}^{2}$ are derived by using MRT and MRC principles as

$$U_i^{(J_{K^{\circledast}})}\Big|_{i=1}^{2}{=}\frac{\left(h_{S_iR_{K^{\circledast}}}^{(J_{K^{\circledast}})}\right)^H}{\left|\left|h_{S_iR_{K^{\circledast}}}^{(J_{K^{\circledast}})}\right|\right|} \text{ and } V_i^{(J_{K^{\circledast}})}\Big|_{i=1}^{2}{=}\frac{\left(h_{S_iR_{K^{\circledast}}}^{(J_{K^{\circledast}})}\right)^{\dagger}}{\left|\left|h_{S_iR_{K^{\circledast}}}^{(J_{K^{\circledast}})}\right|\right|}. (12)$$

The overall outage probability of the joint relay, beamforming and antenna selection can be readily derived by using (6) as

$$P_{out}{=}\prod_{k=1}^{K}\left[\Psi_{N_1,N_2,\zeta_{1,k},\zeta_{2,k}}(\gamma_{th}){+}\Psi_{N_2,N_1,\zeta_{2,k},\zeta_{1,k}}(\gamma_{th})\right]^{N_{R_k}}, (13)$$

where $\Psi_{M,N,a,b}(z)$ is given by (7) after replacing N_R, α, β, η and $\phi(z)$ with N_{R_k}, $\alpha_k = \frac{\bar{\gamma}_S+\bar{\gamma}_{R_k}}{\bar{\gamma}_S\bar{\gamma}_{R_k}}$, $\beta_k = \frac{1}{\bar{\gamma}_{R_k}}$ and $\phi_k(z) = \frac{1}{\bar{\gamma}_S\bar{\gamma}_{R_k}}\sqrt{(\bar{\gamma}_S^2 + \bar{\gamma}_S\bar{\gamma}_{R_k} + \bar{\gamma}_{R_k}^2/4)z^2 + \bar{\gamma}_S\bar{\gamma}_{R_k}z + \frac{z}{2\bar{\gamma}_S}}$, respectively.

The asymptotically exact high SNR approximation of the outage probability for joint relay and antenna selection can be derived as follows:

$$P_{out}^{\infty} = \left(\prod_{k=1}^{K}\Delta_k\right)\left(\frac{\gamma_{th}}{\bar{\gamma}}\right)^{\sum_{k=1}^{K}G_{d_k}}{+}o\left(\bar{\gamma}^{-(\sum_{k=1}^{K}G_{d_k}+1)}\right), (14)$$

where the diversity order G_d is given by

$$G_d = \sum_{k=1}^{K}G_{d_k} = \min(N_1, N_2)\sum_{k=1}^{K}N_{R_k}. \quad (15)$$

In (14), Δ_k can be obtained again by replacing ζ_1, ζ_2 and μ_R of (10) with $\zeta_{1,k}$, $\zeta_{2,k}$ and $\mu_{R_k} = \frac{\bar{\gamma}_{R_k}}{\bar{\gamma}}$, respectively.

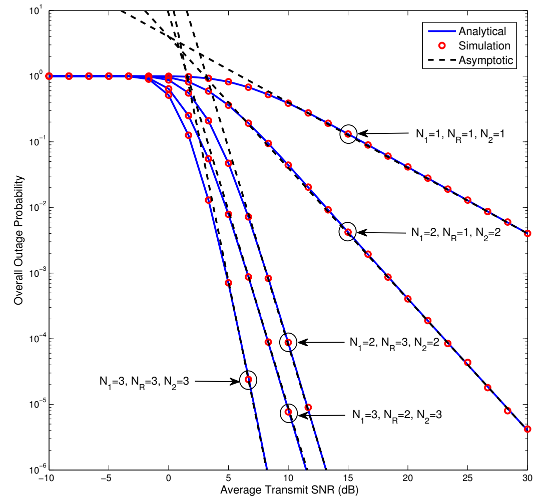

Fig. 1. The overall outage probability of joint beamforming and antenna selection for a single-relay MIMO AF TWRN. The hop distances are modeled as $d_{S_1R} = 2.5d_{S_2R}$ and the path-loss exponent is $\delta = 3.6$.

[6]Similarly, the information outage probability can be defined as follows: $P_{out} = \Pr[\log(1+z) \leq R_{th}] = \Pr\left[z \leq 2^{R_{th}} - 1\right]$, where $z = \min\left(\gamma_{S_1R}^{(J,L,M)}, \gamma_{S_2R}^{(J,L,M)}\right)$.

$$\Psi_{M,N,a,b}(z) = 1 - \sum_{k=0}^{N-1} \frac{a^k b^M \gamma\left(M+k, \frac{(a+b)\beta z}{ab}\right)}{(a+b)^{M+k}\Gamma(M)\Gamma(k+1)} - \sum_{n=0}^{N-1}\sum_{l=0}^{M+n-1} \frac{\binom{M+n-1}{l}(\beta z)^{M+n-l-1} \mathrm{e}^{-\frac{(a+b)\beta z}{ab}} \gamma\left(l+1, \frac{(a+b)\phi(z)}{ab}\right)}{(a+b)^{l+1} a^{M-l-1} b^{n-l-1}\Gamma(M)\Gamma(n+1)}$$
$$- \sum_{n=0}^{N-1}\sum_{p=0}^{n}\sum_{q=0}^{M-1} \frac{\binom{n}{p}\binom{M-1}{q}\alpha^p \beta^{M-q-1} z^{M+n-q-1} (\alpha\beta z + \eta)^{n-p} \mathrm{e}^{-\left(\frac{\beta z + \phi(z)}{a} + \frac{\alpha z}{b}\right)}}{\Gamma(M)\Gamma(n+1) a^{M+n-p-q-1} b^n} \mathcal{I}_{a,b,p+q-n}(z). \quad (7)$$

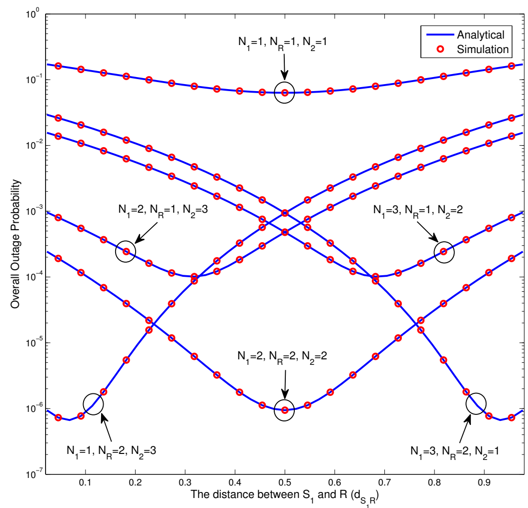

Fig. 2. The overall outage probability verses the relay location. Here, ζ_1 and ζ_2 are modeled as $\zeta_1 = (d_{S_1R})^{-\delta}$ and $\zeta_2 = (d_{S_2R})^{-\delta}$, where $\delta = 2.7$. The transmit SNRs at each terminal is 10 dB.

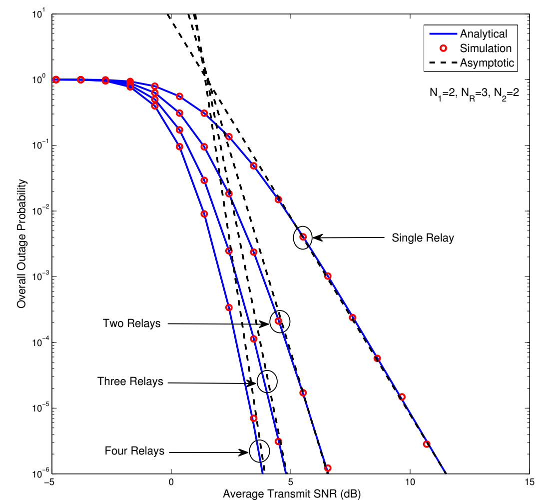

Fig. 3. The overall outage probability of joint relay, beamforming, and antenna selection for MIMO AF TWRN. The hop distances are modeled as $d_{S_1R} = d_{S_2R}$ and the path-loss exponent is $\delta = 3.6$.

VI. Numerical Results

In Fig. 1, the overall outage probability is plotted for a single-relay MIMO AF TWRN. The analytical outage curves corresponding to several antenna set-ups are plotted by using (6) and (8). Further, the outage curve corresponding to a single-antenna TWRN is plotted as a benchmark. Fig. 1 clearly reveals that the MIMO TWRNs with the proposed transmission strategy provide significant gains over the single-antenna TWRNs. For instance, at 10^{-2} outage probability, a triple-antenna TWRN provides a 22.67 dB gain over the single-antenna TWRN. Our high SNR outage approximations are in fact asymptotically exact and provide valuable insights into practical MIMO TWRN design in terms of the diversity order and array gains. The exact match between the Monte-Carlo simulations and the analytical curves validates our derivations.

Fig. 2 studies the effect of relay location on the performance of a single-relay MIMO AF TWRN by plotting the overall outage probability against the distance between S_1 and R. The path-loss dependent parameters ζ_1 and ζ_2 in (6) and (13) as are modeled as $\zeta_1 = (d_{S_1R})^{-\delta}$ and $\zeta_2 = (d_{S_2R})^{-\delta}$, where $\delta = 2.7$ is the path-loss exponent. Here, d_{S_1R} and d_{S_2R} are the distances between $S_1 \to R$ and $S_2 \to R$, respectively, and are modeled to satisfy $d_{S_1R} + d_{S_1R} = 1$. Fig. 2 clearly shows that the optimal relay location, which minimize the overall outage probability, is the half-way point between S_1 and S_2, whenever the antenna configuration at S_1, R and S_2 is symmetric (i.e., $N_1 = N$, $N_R = M$, $N_2 = N$). However, this optimal location shifts toward the source terminal, which has the lowest number of antennas, whenever the antenna configuration at each terminal is asymmetric.

In Fig. 3, the overall outage probability of multi-relay MIMO AF TWRNs with a common antenna configuration (i.e., $N_1 = 3, N_R = 2, N_2 = 3$) is plotted by using (13) and (14). Again, the outage curves corresponding to the single-relay TWRN is plotted as a benchmark to reveal the performance gains of multi-relay TWRNs. Specifically, at 10^{-5} outage probability, the dual-relay TWRN provides a gain of 4.16 dB over that of its single-relay counterpart. However, deploying more than three relays does not yield significant improvements; for example, at 10^{-5} outage probability, only a 0.85 dB gain can be obtained by going from a triple-relay TWRN to a quadruple-relay TWRN.

VII. Conclusion

A novel joint beamforming and antenna selection strategy was proposed and analyzed for single-relay MIMO AF TWRNs based on minimizing the overall outage probability. The performance of this strategy was studied by deriving closed-form expressions for the exact and high SNR approximation of the overall outage probability, and diversity order. Specifically, the multi-relay MIMO TWRNs were also treated by proposing and analyzing a joint beamforming, antenna and relay selection strategy. In particular, the proposed strategies are optimal in the sense of the outage probability, and hence, in the sense of diversity order as well. In fact, the diversity orders of the individual branches accumulate to yield the overall diversity of the multi-relay MIMO TWRNs. Interestingly, the diversity order is proportional to the total number of antennas at all the available relays and minimum of antennas at two sources. Our numerical results reveals valuable insights into practical MIMO TWRN design, for example, in terms of diversity gains and optimal relay locations for various antenna and relay set-ups.

VIII. Appendix

In this appendix, the proofs of the CDF of the effective e2e SNR and its single polynomial approximation are provided.

A. The proof of the CDF of the effective e2e SNR

$$F_Z(z) = \Pr\left[Z = \max_{1\le j\le N_R}\left\{\min\left(\gamma_{S_1}^{(j)}, \gamma_{S_2}^{(j)}\right)\right\} \le z\right], \quad (16)$$

where $\gamma_{S_1}^{(j)}$ and $\gamma_{S_2}^{(j)}$ are defined in (3) and simplified further as follows:

$$\gamma_{S_1}^{(j)} = \frac{X_j Y_j}{\alpha X_j + \beta Y_j + \eta} \text{ and } \gamma_{S_2}^{(j)} = \frac{X_j Y_j}{\beta X_j + \alpha Y_j + \eta}, \quad (17)$$

where $X_j = \left|\left|h_{S_1 R}^{(j)}\right|\right|^2$ and $Y_j = \left|\left|h_{S_2 R}^{(j)}\right|\right|^2$. In (17), $\alpha = \frac{\bar{\gamma}_S + \bar{\gamma}_R}{\bar{\gamma}_S \bar{\gamma}_R}$, $\beta = \frac{1}{\bar{\gamma}_R}$ and $\eta = \frac{1}{\bar{\gamma}_S \bar{\gamma}_R}$, where $\bar{\gamma}_S = \frac{\mathcal{P}_S}{\sigma_S^2}$ and $\bar{\gamma}_R = \frac{\mathcal{P}_R}{\sigma_R^2}$ are the average transmit SNRs at the source terminals and the relay. Without loss of generality, it is assumed that the transmit powers and the AWGN noise variances at both S_1 and S_2 are identical, i.e., $\mathcal{P}_1 = \mathcal{P}_2 = \mathcal{P}_S$ and $\sigma_1^2 = \sigma_2^2 = \sigma_S^2$.

We observe that the random variables $\gamma_{S_1}^{(j)}$ and $\gamma_{S_2}^{(j)}$ are not statistically independent. Now, we start deriving $F_Z(z)$ in (16) by first defining $Z_j \triangleq \min\left(\gamma_{S_1}^{(j)}, \gamma_{S_2}^{(j)}\right)$ and then simplifying it as follows [15]:

$$Z_j = \begin{cases} \gamma_{S_1}^{(j)}, & Y_j \le X_j \\ \gamma_{S_2}^{(j)}, & Y_j > X_j. \end{cases} \quad (18)$$

The CDF of Z_j can be derived as follows [15]:

$$F_{Z_j}(z) = \Pr[Z_j \le z] = \mathcal{F}_1(z) + \mathcal{F}_2(z), \quad (19)$$

where $\mathcal{F}_1(z)$ and $\mathcal{F}_2(z)$ are defined as

$$\mathcal{F}_1(z) \triangleq \Pr\left[\left\{\gamma_{S_1}^{(j)} \le z\right\} \cap \{Y_j \le X_j\}\right] \quad \text{and} \quad (20)$$

$$\mathcal{F}_2(z) \triangleq \Pr\left[\left\{\gamma_{S_2}^{(j)} \le z\right\} \cap \{X_j < Y_j\}\right]. \quad (21)$$

By substituting $\gamma_{S_1}^{(j)}$ in (17) into (20), $\mathcal{F}_1(z)$ can be expressed in a mathematically tractable form as follows:

$$\mathcal{F}_1(z) = \Pr[\{X_j \le \beta z\} \cap \{Y_j \le X_j\}] + \Pr\left[\left\{Y_j \le \frac{z(\alpha X_j + \eta)}{X_j - \beta z}\right\} \cap \{Y_j \le X_j\}\right]. \quad (22)$$

After some mathematical manipulations, $\mathcal{F}_1(z)$ is expanded as

$$\begin{aligned}\mathcal{F}_1(z) &= \int_{x=0}^{\beta z}\int_{y=0}^{x} f_{X_j}(x)\, f_{Y_j}(y)\, \mathrm{d}y\mathrm{d}x \\ &+ \int_{t=0}^{\infty}\Pr\left[Y_j \le \min\left(\frac{z(\alpha(t+\beta z)+\eta)}{t}, t+\beta z\right)\right] f_{X_j}(t+\beta z)\,\mathrm{d}t \\ &= \mathcal{J}_1(z) + \mathcal{J}_2(z) + \mathcal{J}_3(z), \end{aligned} \quad (23)$$

where $\mathcal{J}_1(z)$, $\mathcal{J}_2(z)$ and $\mathcal{J}_3(z)$ are defined as

$$\mathcal{J}_1(z) \triangleq \int_{x=0}^{\beta z}\int_{y=0}^{x} f_{X_j}(x)\, f_{Y_j}(y)\, \mathrm{d}y\mathrm{d}x, \quad (24a)$$

$$\mathcal{J}_2(z) \triangleq \int_{t=0}^{\phi(z)} F_{Y_j}(t+\beta z)\, f_{X_j}(t+\beta z)\,\mathrm{d}t, \text{ and} \quad (24b)$$

$$\mathcal{J}_3(z) \triangleq \int_{t=\phi(z)}^{\infty} F_{Y_j}\!\left(\frac{z(\alpha(t+\beta z)+\eta)}{t}\right) f_{X_j}(t+\beta z)\,\mathrm{d}t. \quad (24c)$$

In (24a), $f_{X_j}(x)$ and $f_{Y_j}(y)$ are the PDFs of X_j and Y_j, respectively, and given by

$$f_{X_j}(x) = \frac{x^{N_1-1}\mathrm{e}^{-\frac{x}{\zeta_1}}}{\Gamma(N_1)\,\zeta_1^{N_1}} \text{ and } f_{Y_j}(y) = \frac{y^{N_2-1}\mathrm{e}^{-\frac{y}{\zeta_2}}}{\Gamma(N_2)\,\zeta_2^{N_2}}. \quad (25)$$

Similarly, in (24b) and (24c), $F_{X_j}(x)$ and $F_{Y_j}(y)$ are the CDFs of X_j and Y_j, respectively, and given by

$$F_{X_j}(x) = \frac{\gamma\left(N_1, \frac{x}{\zeta_1}\right)}{\Gamma(N_1)} \text{ and } F_{Y_j}(y) = \frac{\gamma\left(N_2, \frac{y}{\zeta_2}\right)}{\Gamma(N_2)}. \quad (26)$$

By substituting (25) and (26) into (24a) and (24b), $\mathcal{J}_1(z)$ and $\mathcal{J}_2(z)$ can be evaluated exactly in closed-form as given in first and second terms of (7). However, there appears to have no exact closed-form solution for $\mathcal{J}_3(z)$. Nevertheless, it can be evaluated approximately by using either the Gauss Laguerre quadrature (GLQ) rule [17] or Taylor series expansion techniques as follows:

By substituting (25) and (26) into (24c), $\mathcal{J}_3(z)$ is expanded as

$$\mathcal{J}_3(z) = \sum_{n=0}^{N_2-1}\sum_{p=0}^{n}\sum_{q=0}^{N_1-1}\Theta_{n,p,q}(z)\mathcal{I}_{\zeta_1,\zeta_2,p+q-n}(z), \quad (27)$$

where $\Theta_{n,p,q}(z)$ in (27) is given by

$$\Theta_{n,p,q}(z) = \frac{\binom{n}{p}\binom{N_1-1}{q}a^k b^{N_1}\alpha^p\beta^{N_1-q-1}}{(a+b)^{N_1+k}\Gamma(N_1)\Gamma(k+1)} \times z^{N_1+n-q-1}(\alpha\beta z+\eta)^{n-p}\mathrm{e}^{-\left(\frac{\beta z+\phi(z)}{a}+\frac{\alpha z}{b}\right)}. \quad (28)$$

Further, $I_{\zeta_1,\zeta_2,p+q-n}(z)$ in (27) is given by

$$I_{\zeta_1,\zeta_2,p+q-n}(z) = \int_0^{\infty}\mathcal{A}(t)\mathrm{e}^{-t}\mathrm{d}t, \quad \text{where} \quad (29)$$

$$\mathcal{A}(t) = \left(t+\frac{\phi(z)}{\zeta_1}\right)^{p+q-n}\mathrm{e}^{-\left(\frac{z(\alpha\beta z+\eta)}{\zeta_1\zeta_2\left(t+\frac{\phi(z)}{\zeta_1}\right)}\right)}. \quad (30)$$

1) Evaluation of $I_{\zeta_1,\zeta_2,p+q-n}(z)$ by using GLQ rule [17]:

The integral $I_{\zeta_1,\zeta_2,p+q-n}(z)$ in (29) is in the form of GLQ rule [18, Eq. (25.4.45)]. Thus, it can readily be evaluated as

$$\mathcal{I}_{\zeta_1,\zeta_2,p+q-n}(z) = \sum_{t=1}^{T_g} w_t\mathcal{A}(x_t) + \mathcal{R}_{T_g}, \quad (31)$$

where $x_t|_{t=1}^{T_g}$ and $w_t|_{t=1}^{T_g}$ are the abscissas and weights of the GLQ, respectively [18, Eq. (25.4.45)]. Specifically, x_t is the t-th root of the Laguerre polynomial $\mathcal{L}_n(x)$ [18, Chap. 22] and the corresponding t-th weight is given by $w_t = \frac{(t!)^2 x_t}{(t+1)^2[\mathcal{L}_{t+1}(x_t)]^2}$. In particular, both x_t and w_t can be efficiently computed by using the classical algorithm proposed in [17]. Further, T_g is the number of terms used in the GLQ summation and $\mathcal{R}_{T_g}$ is the remainder term, which readily diminishes as T_g approaches as small as 10 [17].

2) Evaluation of $I_{\zeta_1,\zeta_2,p+q-n}(z)$ by using Taylor series expansion: By first replacing the exponential term of $\mathcal{A}(z)$ in (30) by its Taylor series expansion and then changing the dummy variable of integration as $t+\frac{\phi(z)}{\zeta_1}\to t$, $I_{\zeta_1,\zeta_2,p+q-n}(z)$

can be evaluated by using [18, Eq. (6.5.3)] as

$$\mathcal{I}_{\zeta_1,\zeta_2,p+q-n}(z) = \mathrm{e}^{\frac{\phi(z)}{\zeta_1}} \sum_{i=0}^{\infty} \frac{\left(-\zeta_1 z[\alpha\beta z+\eta]\right)^i}{\zeta_2^i\,(i)!} \times \Gamma\left(p+q-n-j+1, \frac{\phi(z)}{\zeta_1}\right). \quad (32)$$

Now, by following similar steps to those of $\mathcal{F}_1(z)$, $\mathcal{F}_2(z)$ in (21) can be evaluated readily. Then the CDF of Z_j can be derived as $F_{Z_j}(z) = \mathcal{F}_1(z) + \mathcal{F}_2(z)$, which yields the desired result $F_Z(z) = [F_{Z_j}(z)]^{N_R}$ (6).

B. The proof of the high SNR approximation of the overall outage probability

The single polynomial approximation of the CDFs of X_j and Y_j in (26) at the origin can be derived as

$$F_{X_j}^{\infty}(x) = \frac{(x/\zeta_1)^{N_1}}{\Gamma(N_1+1)} + o\left(x^{N_1+1}\right) \quad \text{and}$$
$$F_{Y_j}^{\infty}(y) = \frac{(y/\zeta_2)^{N_2}}{\Gamma(N_2+1)} + o\left(y^{N_2+1}\right). \quad (33)$$

Similarly, the single polynomial approximations of the PDFs of X_j and Y_j at the origin are given by

$$f_{X_j}^{\infty}(x) = \frac{x^{N_1-1}}{\Gamma(N_1)\,\zeta_1^{N_1}} + o\left(x^{N_1}\right) \quad \text{and}$$
$$f_{Y_j}^{\infty}(y) = \frac{y^{N_2-1}}{\Gamma(N_2)\,\zeta_2^{N_2}} + o\left(y^{N_2}\right). \quad (34)$$

First, we consider $\mathcal{F}_1(z)$ in (19). By substituting (34) and (33) into (23), the single polynomial approximations of $\mathcal{J}_1(z)$ and $\mathcal{J}_2(z)$ at the origin can be derived readily as follows:

$$\mathcal{J}_1^{\infty}(z) = \frac{(\beta z)^{N_1+N_2}}{(N_1+N_2)\Gamma(N_1+1)\,\Gamma(N_2)\,\zeta_1^{N_1}\zeta_2^{N_2}} + o\left(z^{N_1+N_2+1}\right),$$
$$\mathcal{J}_2^{\infty}(z) = \frac{(\alpha z)^{N_1+N_2}}{(N_1+N_2)\Gamma(N_1)\,\Gamma(N_2+1)\,\zeta_1^{N_1}\zeta_2^{N_2}} + o\left(z^{N_1+N_2+1}\right). \quad (35)$$

Next, the single polynomial approximations of $\mathcal{J}_3(z)$ at the origin can be derived follows: The Integral $\mathcal{J}_3(z)$ in (24c) can be re-written by applying a change of variable; $t + \beta z \to t$ as

$$\mathcal{J}_3(z) = \int_{t=\phi(z)+\beta z}^{\infty} \Pr\left[Y_j \leq \frac{z(\alpha t+\eta)}{t-\beta z}\right] f_{X_j}(t)\,\mathrm{d}t. \quad (36)$$

Let us consider the single polynomial approximation of $\mathcal{J}_3(z)$ at the origin. If $z \to 0^+$, then $\frac{z(\alpha t+\eta)}{t-\beta z} \to 0^+$. Thus, $\mathcal{J}_3(z)$ in (36) can be approximated at $z \to 0^+$ as follows:

$$\mathcal{J}_3^{\infty}(z) = F_{Y_j}^{\infty}(\alpha z)\left(z \to 0^+ \int_{t=\phi(z)+\beta z}^{\infty} f_{X_j}(t)\,\mathrm{d}t\right)$$
$$= F_{Y_j}^{\infty}(\alpha z)\left[1 - F_{X_j}^{\infty}(\phi(z)+\beta z)\right] \quad (37)$$

By substituting (33) into (37) and by selecting the lowest powers of z, the single polynomial approximation of $\mathcal{J}_3(z)$ at the origin can be derived as

$$\mathcal{J}_3^{\infty}(z) = \frac{(\alpha z)^{N_2}}{\zeta_2^{N_2}} + o\left(z^{N_2+1}\right). \quad (38)$$

Now, the single polynomial approximation of $\mathcal{J}_1(z)$ at the origin is given $\mathcal{F}_1^{\infty}(z) = \mathcal{J}_1^{\infty}(z) + \mathcal{J}_2^{\infty}(z) + \mathcal{J}_3^{\infty}(z)$. In particular, the behavior of $\mathcal{F}_1(z)$ at the origin is completely governed by $\mathcal{J}_3^{\infty}(z)$ as it has the lowest powers of z, and consequently $\mathcal{F}_1^{\infty}(z)$ can be simplified as

$$\mathcal{F}_1^{\infty}(z) = \frac{(\alpha z)^{N_2}}{\zeta_2^{N_2}} + o\left(z^{N_2+1}\right). \quad (39)$$

By following similar steps to those of $\mathcal{F}_1^{\infty}(z)$, the single polynomial approximation of $\mathcal{F}_2(z)$ in (19) at the origin can be derived as

$$\mathcal{F}_2^{\infty}(z) = \frac{(\alpha z)^{N_1}}{\zeta_1^{N_1}} + o\left(z^{N_1+1}\right). \quad (40)$$

Next, the single polynomial approximation of Z_j at the origin can be derived by using (39) and (40) as follows:

$$F_{Z_j}^{\infty}(z) = \mathcal{F}_1^{\infty}(z) + \mathcal{F}_2^{\infty}(z). \quad (41)$$

Now, the asymptotic outage probability can be derived as in (8) by first obtaining the single polynomial approximation of Z at the origin by substituting (41) into $F_Z^{\infty}(z) = (F_{Z_j}^{\infty}(z))^{N_R}$ and then evaluating it at γ_{th}.

REFERENCES

[1] S. Berger *et al.*, "Recent advances in amplify-and-forward two-hop relaying," *IEEE Commun. Mag.*, vol. 47, no. 7, pp. 50–56, Jul. 2009.

[2] B. Rankov and A. Wittneben, "Spectral efficient protocols for half-duplex fading relay channels," *IEEE J. Sel. Areas Commun.*, vol. 25, no. 2, pp. 379–389, 2007.

[3] Y. Han *et al.*, "Performance bounds for two-way amplify-and-forward relaying," *IEEE Trans. Wireless Commun.*, vol. 8, no. 1, pp. 432–439, Jan. 2009.

[4] R. H. Y. Louie, Y. Li, and B. Vucetic, "Practical physical layer network coding for two-way relay channels: performance analysis and comparison," *IEEE Trans. Wireless Commun.*, vol. 9, pp. 764–777, 2010.

[5] R. Zhang *et al.*, "Optimal beamforming for two-way multi-antenna relay channel with analogue network coding," *IEEE J. Sel. Areas Commun.*, vol. 27, no. 5, pp. 699–712, 2009.

[6] C. Li, L. Yang, and W.-P. Zhu, "Two-way MIMO relay precoder design with channel state information," *IEEE Trans. Commun.*, vol. 58, no. 12, pp. 3358–3363, 2010.

[7] A. Y. Panah and R. W. Heath, "MIMO two-way amplify-and-forward relaying with imperfect receiver CSI," *IEEE Trans. Veh. Technol.*, vol. 59, no. 9, pp. 4377–4387, 2010.

[8] J. Joung and A. Sayed, "Multiuser two-way amplify-and-forward relay processing and power control methods for beamforming systems," *IEEE Trans. Signal Process.*, vol. 58, no. 3, pp. 1833–1846, Mar. 2010.

[9] X. Wang and X.-D. Zhang, "Optimal beamforming in MIMO two-way relay channels," in *IEEE Global Telecommun. Conf.*, Dec. 2010, pp. 1–5.

[10] T. M. Kim, B. Bandemer, and A. Paulraj, "Beamforming for network-coded MIMO two-way relaying," in *44th ASILOMAR Conf. Signals, Systems and Computers*, Nov. 2010, pp. 647–652.

[11] P. Dighe, R. Mallik, and S. Jamuar, "Analysis of transmit-receive diversity in Rayleigh fading," *IEEE Trans. Commun.*, vol. 51, no. 4, pp. 694–703, Apr. 2003.

[12] A. F. Molisch and M. Z. Win, "MIMO systems with antenna selection," *IEEE Microw. Mag.*, vol. 5, no. 1, pp. 46–56, 2004.

[13] M. Eslamifar *et al.*, "Performance analysis of two-way multiple-antenna relaying with network coding," in *Proc. IEEE 70th Vehicular Technology Conf. Fall*, 2009, pp. 1–5.

[14] ——, "Max-min antenna selection for bi-directional multi-antenna relaying," in *Proc. IEEE 71st Vehicular Technology Conf.*, 2010, pp. 1–5.

[15] G. Amarasuriya, C. Tellambura, and M. Ardakani, "Two-way amplify-and-forward MIMO relay networks with antenna selection," in *IEEE Global Commun. Conf. (GLOBCOM)*, Houston, Texas, USA, Dec. 2011, pp. 1–5.

[16] D. N. C. Tse, P. Viswanath, and L. Zheng, "Diversity-multiplexing tradeoff in multiple-access channels," *IEEE Trans. Inf. Theory*, vol. 50, no. 9, pp. 1859–1874, 2004.

[17] Golub *et al.*, "Calculation of Gauss quadrature rules," Stanford, CA, USA, Tech. Rep., 1967.

[18] M. Abramowitz and I. Stegun, *Handbook of Mathematical Functions*. Dover Publications, Inc., New York, 1970.